

# Investigation of Grid Supply Harmonic Effects in Wound Rotor Induction Machines

Nur Sarma, Paul M. Tuohy, Siniša Djurović

**Abstract**—This paper presents an in-depth investigation of the effects of several grid supply harmonic voltages on the stator currents of an example wound rotor induction machine. The observed effects of higher order grid supply harmonics are identified using a finite element time stepping transient model, as well as a time-stepping electromagnetic model. In addition, a number of analytical equations to calculate the spectral content of the stator currents are presented in the paper. The presented equations are validated through comparison with the obtained spectra predicted using the finite element and electromagnetic models. The presented study provides a better understanding of the origin of supply harmonic effects identified in the stator currents of the example wound rotor induction machine. Furthermore, the study helps to understand the effects of higher order supply harmonics on the harmonic emissions of the wound rotor induction machine.

**Keywords**—Wound rotor induction machine, supply harmonics, current spectrum, power spectrum, power quality, harmonic emissions, finite element analysis.

## I. INTRODUCTION

INDUCTION machines are widely used in numerous industries due to their simplicity, reliability and relative inexpensiveness. With the increase in the development and deployment of electrical transport systems such as electric vehicles and renewable power generation systems such as wind turbines (WTs), induction machines have also been employed in these areas and are therefore receiving increased research attention [1], [2].

The application of wound rotor induction machines (WRIMs) has particularly increased with the growth in the number of installed WTs, since WRIMs are used in the doubly fed induction generator (DFIG) topology as a variable speed WT configuration. The DFIG is currently the most common type of installed WT configuration, since the output power of the generator can be easily controlled [3], [4]. However, DFIGs produce harmonic emissions, which are a known power quality concern. Therefore, WTs have to fulfill a number of power quality requirements before being connected to an electrical grid such as the harmonic content of the generated current, which are regulated by relevant standards [5].

The electrical grids that supply WTs are a known source of harmonics and are one of the main causes of harmonic

distortion in WTs [6]-[8]. This is because the WRIM requires voltage excitation from the grid. The voltage excitation is necessary for the operation of the WRIM but results in additional harmonic distortion in the generated current and consequently, power quality issues [8].

These grid supply harmonics produce stator current harmonics, which can cause torque pulsations and hence, mechanical vibration in the WRIM that may lead to mechanical faults and premature failure of WT components [9]. Furthermore, the grid supply harmonics can increase the core and copper losses and thus, reduce the efficiency of the WRIM [10]. It is to be noted that there are other sources of harmonics in WRIMs, i.e. the MMF space harmonics. These are caused by the rotor and stator windings being housed in discrete slots and therefore give rise to higher order harmonics in the air-gap magnetic flux. Slotting harmonics are another source of harmonics and are produced due to the variations in reluctance caused by the stator and rotor slots, which are specific to the design of each electric machine. Although all these sources of harmonics have effects on the WRIM signals spectra, the objective of this paper is to highlight the effects of the grid supply harmonic specifically.

It is important to achieve a deep understanding of the operation of WRIMs and also what type of changes occurs in the spectrum of the electrical and mechanical variables with the existing grid supply harmonics in order to minimize the negative effects of these higher order supply harmonics on the grids that are coupled to WTs and also the WT drivetrain components themselves. As a result, comprehensive machine modeling techniques such as finite element analysis (FEA) and time-stepping electromagnetic models have gained significant importance, since they allow in-depth investigation of harmonic analysis in electrical power systems for power quality studies [11]. This paper will therefore investigate the effects of grid supply harmonics on the stator currents of an example WRIM using both a FE model and a conductor distribution function (CDF) model as a time-stepping electromagnetic model.

The remainder of the paper is presented as follows: in Section II, the modelling of a WRIM using both a FE model and a CDF model will be described. Section III provides generalized equations to calculate possible stator current frequency components, which are compared with the results from the model simulations in Section IV. Finally, the conclusions of the paper are provided in Section V.

## II. MODELING OF A WRIM

Representation of harmonic effects is becoming increasingly

Nur Sarma is with Düzce Üniversitesi, Mühendislik Fakültesi, Elektrik Elektronik Mühendisliği, Düzce, Turkey (e-mail: nursarma@duzce.edu.tr).

Paul M. Tuohy is with the University of Manchester, School of Electrical and Electronic Engineering, Power and Energy Division, Manchester, UK.

Siniša Djurović is with the University of Manchester, School of Electrical and Electronic Engineering, Power and Energy Division, Manchester, UK (e-mail: paul.tuohy-2@manchester.ac.uk).

important for improved electric machine behavior and power systems analysis. Today, most of the electric machine modelling techniques used in the literature, i.e.  $dq$  and  $abc$  machine models [12], [13] are not sufficient for detailed frequency domain analysis of electric machine electrical variables, since these modelling techniques assume linearity and only take into account a sinusoidal MMF distribution. Therefore, harmonic machine modeling techniques such as FEA and CDF methods have received increased research attention [14]. This is because both FEA and CDF methods allow representation of time and space harmonic effects in the electrical and mechanical signals of the modeled electric machine.

In the following subsections, the development of the WRIM model using CDF, as well as FEA methods will be described.

#### A. Conductor Distribution Function Model

This subsection presents a brief summary of utilizing CDF methods to develop a WRIM model. CFD models use a coupling impedance approach based on the principles of generalized harmonic analysis, to develop a mathematical model of a WRIM [15]. This modeling technique requires standard WRIM electromechanical model equations to be embedded in time-stepping numerical integration algorithms that are solved using specialist software. The time-stepping numerical integration algorithms require the combination of each individual air-gap field harmonics contribution to the resulting harmonic field effects at each time step. There have been implementations of CDF methods to develop WRIM models using MATLAB and Simulink in the literature, which have previously been presented in [15] and [11], respectively.

The CDF modelling technique enables the representation of a number of arbitrary electrical connections of WRIM windings. A winding is defined as any series connected set of coils. Also, the geometry and design specifications are required as input variables. This provides flexibility to develop arbitrary designed WRIM models and also allows the investigation of WRIM behavior analysis under balanced and unbalanced electrical connections.

The conventional electro-mechanical machine equations to develop a WRIM model utilizing CDF methods in matrix form are written as [11]:

$$[V] = [R][I] + \frac{d[L][I]}{dt} \quad (1)$$

$$T_e - T_{load} = J \frac{d\omega_{mech}}{dt} \quad (2)$$

$$T_e = \frac{1}{2} [I]^T \frac{d[L]}{d\theta_{mech}} [I] \quad (3)$$

$$\omega_{mech} = \frac{d\theta_{mech}}{dt} \quad (4)$$

where:  $[V]$  is the machine voltage vector,  $[I]$  is the machine current vector,  $[R]$  is the machine resistance matrix,  $[L]$  is the

machine inductance matrix,  $T_e$  is the machine electromagnetic torque,  $T_{load}$  is the machine load torque,  $J$  is the rotor inertia,  $\omega_{mech}$  is the rotor mechanical speed, and  $\theta_{mech}$  is the rotor mechanical angle.

The accurate calculation of  $[L]$  is important for modelling a WRIM utilizing CDF methods so that values of harmonics are precisely calculated. This calculation is given for an arbitrary stator/rotor winding  $x$  and an arbitrary stator/rotor winding  $y$  as [15]:

$$L_{x,y} = D \sum_{v=-\infty}^{v=\infty} k_{sk}^v \frac{\bar{C}_x^v \bar{C}_y^v}{v^2} e^{-j\left(\frac{2v\beta(t)}{d}\right)} \quad (5)$$

$$D = \frac{\mu_0 w \pi d^3}{2g} \quad (6)$$

$$\bar{C}_x^v = -j \frac{2}{\pi d} k_b \sum_i k_{pi}^v e^{j\left(\frac{v\theta_i}{d}\right)} \quad (7)$$

where:  $w$  is the stack length [m],  $d$  is the mean air-gap diameter [m],  $g$  is the air-gap length [m],  $\mu_0$  is the permeability of air,  $\beta(t)$  is the rotor displacement from an arbitrary reference position,  $v$  is the harmonic number,  $k_{sk}$  is the skew factor,  $\bar{C}_x$  is harmonic complex conductor distribution of an arbitrary winding  $x$ ,  $k_b$  is the slot mount width factor and  $k_{pi}$  is the pitch factor of  $i^{th}$  coil of winding  $x$ .

Equations (5)-(7) show that the harmonic inductances of the modeled WRIM are calculated at each time step for the existing rotor position and then, the calculated inductance values for each harmonic are summed to calculate the total inductance value for each identified winding. The calculated inductance value is subsequently used in (1) and (3) for further calculations. The WRIM model equations given in (1)-(7) can be solved using an appropriate time-stepping iterative procedure. The detailed mathematical model implementation of the CDF method for a WRIM model can be referred to in [11], [15].

#### B. Finite Element Model

A FE model of the WRIM was built using the Flux2D software package in this work to verify the CDF model, as shown in Fig. 1. 2-D FE modelling rather than 3-D was used, as it has been shown to be sufficiently accurate in previous work [14].

The FE model assumes a balanced three-phase supply. However, to implement additional stator supply harmonics in the FE model, extra voltage sources were added to the electrical coupled circuit. These extra voltage sources were added into each phase as an additional series component, as shown in Fig. 2. These additional voltages sources were modified in each subsequent model with the relevant harmonic voltages required, as will be explained in Section IV.

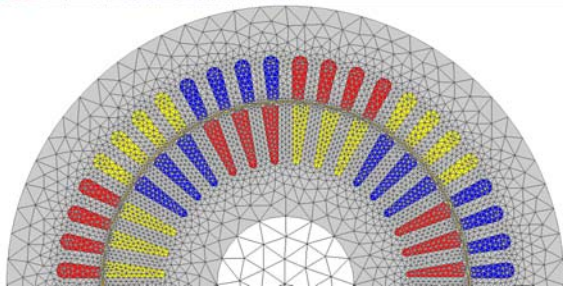


Fig. 1 WRIM FE model

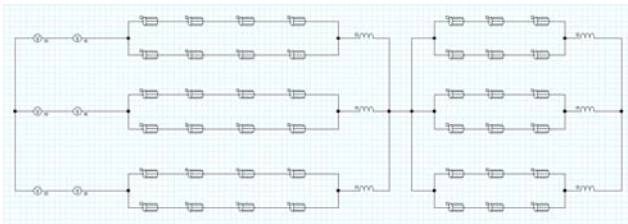


Fig. 2 WRIM FE model coupled circuit schematic with additional series voltage sources

### III. SPECTRAL CONTENT OF THE CURRENT AND POWER SIGNALS

This section presents generalized equations to calculate the numeric values of the possible stator current frequencies of a three-phase,  $p$  pole-pair WRIM operating with higher order harmonic content in the stator supply. The derivation of these equations has been presented in previous works [9], [15] and will therefore not be derived here again.

TABLE I  
 EQUATION TO CALCULATE STATOR CURRENT HARMONICS

Stator Current Harmonics
$f_c^{k,i} =  i \pm 6k(1-s) f$

$f_c$  is the stator current frequencies of interest,  $i$  is the stator supply induced harmonic order number ( $i = 1, 2, 3, \dots$ ),  $s$  is the fractional slip, and  $k$  is the air-gap field pole-pair number ( $k = 0, 1, 2, \dots$ ).

The presented equations in Table I are derived to calculate the frequency components of a WRIM operating with balanced stator and rotor windings, as well as a symmetrical three-phase supply. Furthermore, the operating speed of the machine is assumed to be constant. The equations in Table I show that each higher order supply harmonic creates a range of slip dependent interharmonic frequency components in the stator current that cause harmonic distortion. It is stated in [8] that the magnitudes of these frequency components are related to each specific electric machine's design parameters.

The frequency components calculated using the equations given in Table I for  $i = 1$  originate from a design characteristics of WRIMs [8].

### IV. RESULTS

The ability of both the CDF and FE modeling techniques to represent the grid supply harmonic effects in the electrical signals of the WRIM will be investigated in this section. Furthermore, the capacity of the equations presented in section

III to precisely calculate the higher order supply harmonic effects is also analyzed using the results from both models. The individual higher order supply harmonic effect on the stator currents is studied in turn in this section.

According to European standards, all higher order grid supply harmonics components can be detected such as the 2<sup>nd</sup>, 3<sup>rd</sup>, 5<sup>th</sup>, 7<sup>th</sup>, 9<sup>th</sup>, 11<sup>th</sup> and 13<sup>th</sup> harmonics [16]. As an example, the presented study includes only the 3<sup>rd</sup> and 5<sup>th</sup> harmonic orders for illustration purposes in this work [8]. The magnitudes of these harmonics are set according to the grid code and therefore the values used in the models were set as a percentage of the fundamental such that:

- 3<sup>rd</sup> order harmonic = 5% of the fundamental,
- 5<sup>th</sup> order harmonic = 6% of the fundamental.

These supply harmonics are separately introduced into the FEA and CDF models by superimposing these harmonic voltages onto the fundamental supply frequency.

Both the CDF and FE models were built from the parameters of an industrial 30 kW, 4-pole WRIM [15]. The stator has 48 slots and the rotor has 36 slots. Rotor skew was not considered, and the models were simulated at a constant speed, i.e. speed ripped effects were ignored. An arbitrary operating point of 1,550 rpm was used in the simulations.

The stator windings of the WRIM were assumed to be fed directly from the grid whereas the rotor windings of the WRIM were short-circuited. During the modelling, it was also assumed that the magnitudes and phase angles of all the three-phase harmonic voltage systems were balanced.

The time step of the CDF model was set to 1/10 ms in the simulations, and the obtained results data were processed in MATLAB using the FFT function with a  $2^{17}$  point window length. The FE model time-step was set to 0.167 ms, which is equivalent to a 6,000 Hz sampling rate. This had been shown in previous work to be the optimal value to produce sufficient accuracy whilst also minimizing computational time [14]. The presented results are normalized with respect to the fundamental harmonic components. Furthermore, a 0-1000 Hz bandwidth was chosen to be evaluated. The model results for the A-phase stator current spectra are presented in Figs. 3-8. (The B- and C-phase stator current spectra are not included here, as they show practically the same results).

Figs. 3-5 show the signals spectra of the A-phase stator current when only the fundamental, the 3<sup>rd</sup> and also the 5<sup>th</sup> supply harmonics were modelled using both the FE and CDF models. The presented results show good agreement with each other in the frequency domain to represent higher order supply harmonic effects. The stator current spectrum of both the model results contains spectral components to present effects of stator supply harmonic voltages. However, it is important to highlight that the FE model simulations are extremely computationally intensive compared to the CDF model. For example, obtaining a single transient solution typically requires a time period of  $\approx 15$  hours for the FE model (for the used mesh density and time step size), whereas the time-step model only requires  $\approx 2$  hours in order to achieve the same predicted FFT results presented in Figs. 3-5.

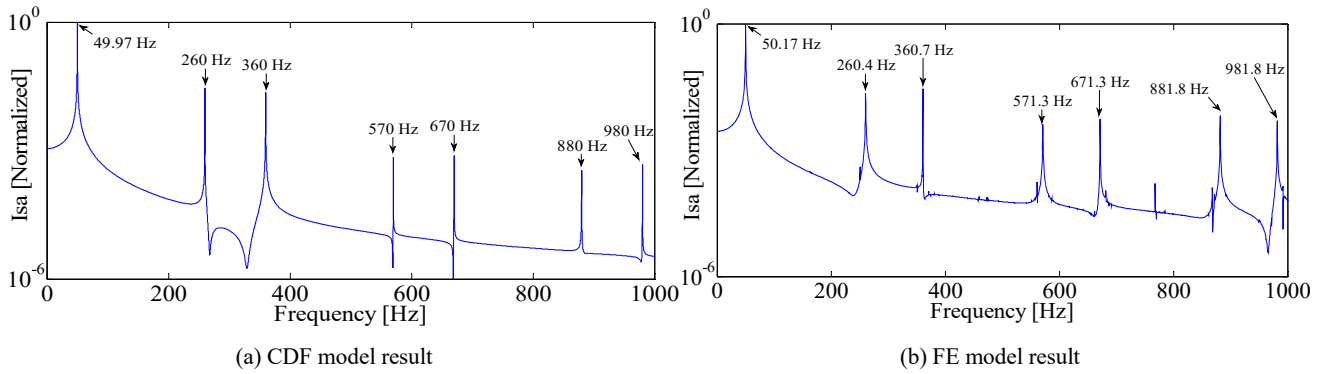


Fig. 3 A-phase stator current spectrum from the CDF and FE models for only the fundamental supply harmonic

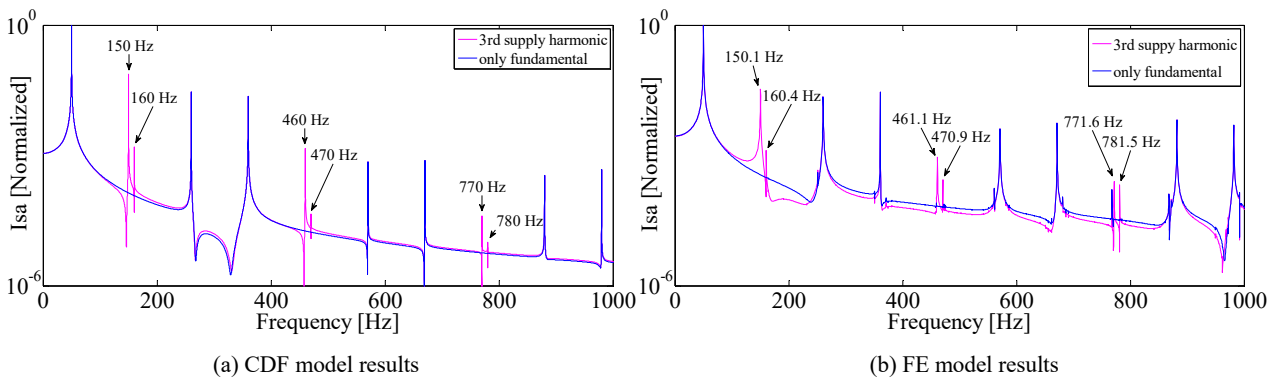
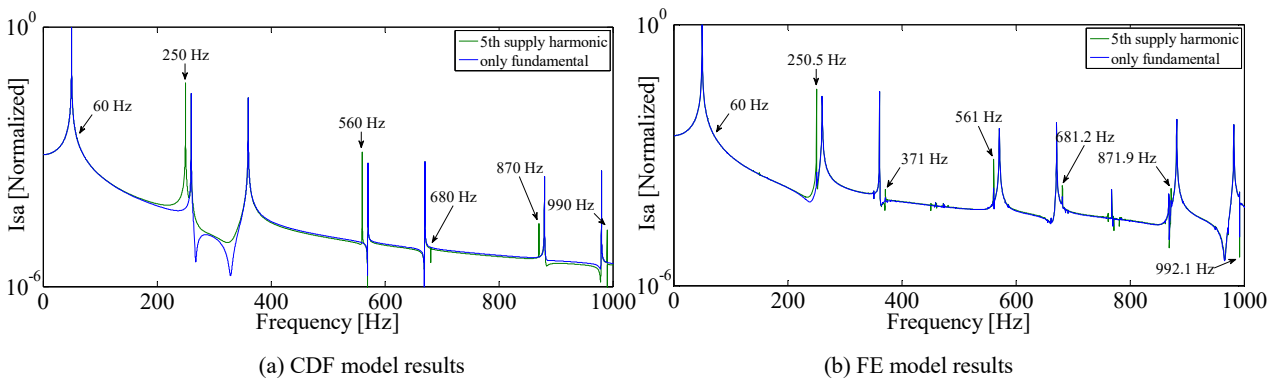


Fig. 4 A-phase stator current spectrum from the CDF and FE models for the fundamental and 3<sup>rd</sup> order supply harmonics



A-phase stator current spectrum from the CDF and FE models for the fundamental and 5<sup>th</sup> order supply harmonics

Fig. 3 shows that the A-phase stator current signal spectra contains a set of interharmonic components (also calculated in Table II) when the WRIM operates with only the fundamental supply frequency. These interharmonic components are due to the slotting effects, and exist in each machine design regardless of geometry, etc. In addition, Figs. 4-5 show that the spectrum of the A-phase stator current also contains a range of harmonic and interharmonic components alongside of the fundamental component shown in Fig. 3. These frequency components are caused by the stator supply harmonic voltages.

All the frequency components identified in the spectrum of the A-phase stator current can be calculated using the equation in Table I for the considered arbitrary operating speed of  $1,550 \text{ rpm}$  ( $s = -0.033$ ), which are calculated and presented in

Table II.

The frequencies in Tables II are calculated by substituting a corresponding operating speed, the value of the examined supply harmonic orders ( $i = 1, 3, 5$ ) and the air-gap magnetic field pole-pair number ( $k = 0, 1, 2, 3$ ) into the presented equation in Table I. The reported frequency components in Table II are used to validate the accuracy of the both models to represent the higher order supply harmonic effects.

## V. CONCLUSIONS

This paper presents a detailed investigation of the effects of stator supply harmonic voltages on the steady-state spectral content of the stator phase currents of a WRIM utilizing finite element and time-stepping electromagnetic modeling

principles. The investigation shows that higher order harmonics in the stator supply result in an increase in the number of harmonics and interharmonic components in the examined signal spectrum. This work verifies that both modelling techniques are able to effectively be used to investigate supply induced harmonic effects in electric machines. In addition, analytical equations that can be used to calculate stator supply induced harmonics and interharmonic components, which are dependent on operating speed, were also provided in the paper.

TABLE II  
STATOR CURRENT FREQUENCY COMPONENTS

<i>i</i>	<i>k</i>	Value (Hz)
1	0	50
1	1	259.9 & 359.9
1	2	569.8 & 669.8
1	3	879.7 & 979.7
3	0	150
3	1	159.9 & 459.9
3	2	469.8 & 769.8
3	3	779.7 & 1079.7
5	0	250
5	1	59.9 & 559.9
5	2	369.8 & 869.8
5	3	679.7 & 1179.7
5	4	989.6 & 1389.6

Each individual supply harmonic creates a corresponding harmonic, as well as a set of interharmonic frequency components in the current spectrum, which create power quality and harmonic emissions issues. These issues can be more important when a WT is connected to a weak network/grid. This paper produced a basis for investigation of the stator supply harmonic voltages effects. Further investigations using other machine signals, and experimentally validated will be reported in future work.

#### REFERENCES

[1] Boglietti, A.; El-Refaie, A.; Drubel, O.; Omekanda, A.; Bianchi, N.; Agamloh, E.; Popescu, M.; Di Gerlando, A.; Borg Bartolo, J., "Electrical Machine Topologies: Hottest Topics in the Electrical Machine Research Community," *Industrial Electronics Magazine*, IEEE, vol.8, no.2, pp.18-30, June 2014.

[2] Agamloh, E. B.; Cavagnino, A., "High efficiency design of induction machines for industrial applications," *Electrical Machines Design Control and Diagnosis (WEMDCD)*, 2013 IEEE Workshop on, pp.33-46, 11-12 March 2013.

[3] M. Edrah, K. L. Lo and O. Anaya-Lara, "Impacts of High Penetration of DFIG Wind Turbines on Rotor Angle Stability of Power Systems," *IEEE Transactions on Sustainable Energy*, vol. 6, no. 3, pp. 759-766, 2015.

[4] S. Heier, *Grid Integration of Wind Energy Onshore and Offshore Conversion Systems*. 3ed. John Wiley & Sons, 2014.

[5] *Wind Turbine Generator Systems - Part 21: Measurement and assessment of power quality characteristics of a grid connected wind turbines*, IEC 61400-21, Aug. 2008.

[6] L. Shi, S. Sun, L. Yao, Y. Ni, and M. Bazargan, "Effects of wind generation intermittency and volatility on power system transient stability," *IET Renewable Power Generation*, vol. 8, no. 5, pp. 509-521, 2014.

[7] M. Bradt, B. Badrzadeh, E. Camm, D. Mueller, J. Schoene, T. Siebert, T. Smith, M. Starke, and R. Walling, "Harmonics and resonance issues in wind power plants," in *Proc. 2011 IEEE Power and Energy Society General Meeting*, pp. 1-8.

[8] S. Djurović, S. Williamson, "Influence of Supply Harmonic Voltages on

DFIG Stator Current and Power Spectrum", *The XIX International Conference on Electrical Machines - ICEM 2010, Rome, 2010*, pp. 1-6.

[9] S. Djurović, D. S. Vilchis-Rodriguez and A. C. Smith, "Supply Induced Interharmonic Effects in Wound Rotor and Doubly-Fed Induction Generators," *IEEE Transactions on Energy Conversion*, vol. 30, no. 4, pp. 1397-1408, 2015.

[10] L. Ching-Yin and L. Wei-Jen, "Effects of nonsinusoidal voltage on the operation performance of a three-phase induction motor," *IEEE Transactions on Energy Conversion*, vol. 14, no. 2., pp. 193-201, June 1999.

[11] N. Sarma, K. Tshiloz, D. S. Vilchis-Rodriguez and S. Djurović, "Modelling of induction machine time and space harmonic effects in the SIMULINK environment," *2015 IEEE International Electric Machines & Drives Conference (IEMDC)*, Coeur d'Alene, ID, 2015, pp. 1279-1285.

[12] A. Junyent-Ferré, O. Gomis-Bellmunt, A. Sumper, M. Sala and M. Mata, "Modeling and control of the doubly fed induction generator wind turbine," *Simulation Modelling Practice and Theory*, vol. 18, no. 9, pp. 1365-1381, 2010.

[13] Y. Liao, L. Ran, G. A. Putrus and K. S. Smith, "Evaluation of the Effects of Rotor Harmonics in a Doubly-Fed Induction Generator With HarmonicInduced Speed Ripple," *IEEE Transactions on Energy Conversion*, vol. 18, no. 4, pp. 508-515, 2003.

[14] P. M. Tuohy, S. Djurović and A. C. Smith, "Finite element analysis of winding fault effects in a wound-rotor induction machine with experimental validation," *6th IET International Conference on Power Electronics, Machines and Drives (PEMD 2012)*, Bristol, 2012, pp. 1-6.

[15] S. Djurović, S. Williamson, A. Renfrew, "Dynamic Model for Doubly-fed Induction Generators with Unbalanced Excitation, both With and Without Faults", *IET Electric Power Applications*, Vol. 3, Iss. 3, pp. 171-177, 2009.

[16] Y. Liao, L. Ran, G. A. Putrus and K. S. Smith, "Evaluation of the Effects of Rotor Harmonics in a Doubly-Fed Induction Generator With HarmonicInduced Speed Ripple," *IEEE Transactions on Energy Conversion*, vol. 18, no. 4, pp. 508-515, 2003.